Structure of Rb-III: Novel Modulated Stacking Structures in Alkali Metals

R. J. Nelmes, M. I. McMahon, J. S. Loveday, and S. Rekhi

Department of Physics and Astronomy and Centre for Science at Extreme Conditions,
The University of Edinburgh, Mayfield Road, Edinburgh EH9 3JZ, United Kingdom

The crystal structure of Rb-III, stable between 13 and 17 GPa, has been determined from quasi-single-crystal x-ray diffraction data. It is orthorhombic, space group $C222_1$, with 52 atoms in the unit cell, and has an 8-10-8-8-10-8 stacking of 8- and 10-atom layers. The recently reported 84-atom structure of Cs-III can be understood as an 8-8-10-8-8-8-8-10-8-8 stacking of the same layers. These represent a new class of modulated elemental structures.

The heavy alkali metals exhibit structural phase transitions from high-symmetry high-coordination cubic phases (bcc and fcc) to more complex low-symmetry phases associated with pressure induced *s*-to-*d* electron transfer. In the case of cesium, the sequence of transitions [1] at relatively low pressures, with five phases up to 12 GPa, and the very unusual isostructural fcc $\rightarrow$ fcc Cs-II to Cs-III transition reported at 4.2 GPa [2] have stimulated a wide range of studies using resistivity, optical, computational, and diffraction techniques [3]. There have been fewer studies of rubidium, with its higher transition pressures, but a similarly complex structural behavior is emerging. The known phase transition sequence is bcc Rb-I to fcc Rb-II at 7 GPa [1], to unknown Rb-III at 13 GPa [1], to incommensurate Rb-IV at 17 GPa [4], to body-centered tetragonal Rb-V at 20 GPa [5] and finally to orthorhombic Rb-VI at 48 GPa [6,7]. It is only very recently that the complex structures of Rb-IV [4,8] and Rb-VI [6] have been determined. The structure of Rb-III remains still unknown. Olijnyk and Holzapfel [5] reported a complex diffraction pattern for Rb-III in 1983 which they were unable to index uniquely. More recent work gave a list of observed *d*-spacings but again no structure solution was obtained [7]. Cs-III has recently been shown *not* to have the same fcc structure as Cs-II, but a remarkable 84-atom C-centered orthorhombic structure [9]. Rb-III and Cs-III mark the transition from simple to complex structures in each system, and there is particular interest in solving Rb-III so that the two may be compared. We report a study of Rb-III using quasi-single-crystal diffraction techniques, and find it to have an orthorhombic structure closely related to that of Cs-III [9].

Experiments were done with high-purity Rb samples from the Aldrich Chemical Company, using Merrill-Bassett diamond-anvil pressure cells (DACs) with tungsten gaskets. All samples were loaded in a dry oxygen-free atmosphere (<1 ppm O_2 and <1 ppm H_2O) to prevent oxidation. A small chip of ruby was used for pressure measurement [10]. To avoid possible contamination, no pressure-transmitting medium was used. Initial powder diffraction data were collected on station 9.1 at SRS, Daresbury Laboratory, using angle-dispersive techniques with an image-plate area detector [11] and a wave-length of 0.4654 Å. Diffraction patterns collected in the low-pressure bcc (Rb-I) and fcc (Rb-II) phases showed no discernible contaminant peaks, confirming the samples to be pure Rb.

On increasing pressure through the Rb-II $\rightarrow$ Rb-III phase transition at 13.2(1) GPa, all samples were found to recrystallize, giving 2D diffraction patterns of Rb-III that were highly textured and "spotty." Despite azimuthal integration [11], different samples were found to give very different peak intensities. In addition, the strongly textured patterns meant that it was not possible to locate the weak low-angle peaks essential for *ab initio* indexing with any confidence. The powder profiles were thus unsuitable for either indexing or structure solution—as previously found [5,7]. However, by raising the pressure directly from Rb-II into Rb-III in one step, we obtained a sample that recrystallized to give clear layer lines of Bragg reflections, as shown in Fig. 1.
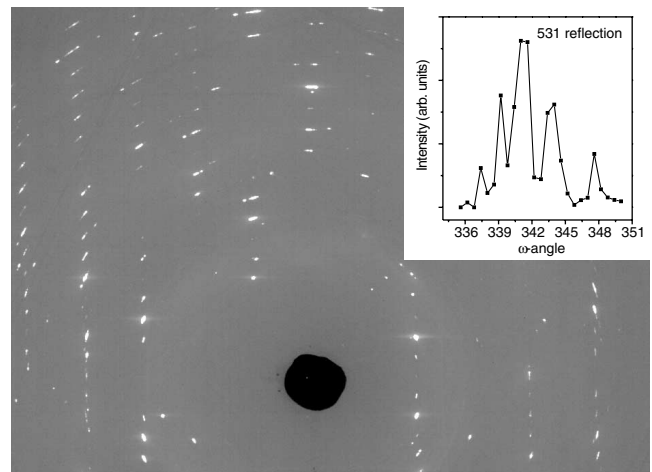

FIG. 1. An image-plate diffraction pattern from a sample of Rb-III at 14.3 GPa. The layer lines of reflections are clearly visible. Reflections are up to a few degrees wide in the plane of the image. The inset shows the much larger width of a scan through the (531) multicrystallite reflection along a direction approximately perpendicular to the plane of the image. The broader features at 341° and 344° each comprise two nearly overlapping peaks.

A series of such images was collected on station 9.1 in 3° steps about a crystal rotation axis (ω). These revealed the reflections to be *much* broader in the direction approximately perpendicular to the plane of the image, having a full width of $\omega \sim 10°-12°$, compared to $\sim 1°$ for the sample used in our recent study of Cs-III [9]. The data were all converted into reciprocal space coordinates, and each reflection then appeared as a $\sim 10°-12°$ arc. The near overlap of adjacent arcs made it impossible to index them using available software, but manipulation of the array of arcs in the viewing software RLATT [12] enabled us to interpret them in terms of a three-dimensional reciprocal lattice that could be hand-indexed on a C-face-centered orthorhombic unit cell with lattice parameters $a = 7.88$ Å, $b = 11.23$ Å, and $c = 18.42$ Å at 14.3 GPa [13].

The indexed reflections revealed systematic absences consistent with space group $C222_1$, the same as for Cs-III [9]. In addition, the similarity of the b/a ratio (1.43) to that of Cs-III (1.435) [9] suggests some relationship between the crystal structures. The measured densities of Rb-II and Rb-IV constrain the number of atoms (Z) in the unit cell to be between 50 and 54, and the $C222_1$ symmetry requires Z to be a multiple of four. Thus, there are 52 atoms in the unit cell, compared with 84 in Cs-III. This difference is reflected in the relatively much smaller c-axis dimension in Rb-III ($c = 34.203$ Å in Cs-III).

To overcome the poor signal:noise ratio arising from the extreme width of the Rb-III reflections, data were collected on station 9.8 at SRS, Daresbury Laboratory using a Brucker Platform diffractometer equipped with a SMART 1K charge-coupled device detector [14]. The x-ray wavelength was 0.4815(1) Å. Data were collected in a series of ω-scans with the stationary detector first covering 0 to 42° in 2θ and then 0 to $-42°$. Each frame of the scans had a width of 0.6° in ω, and an exposure time of 5 s.

One of these scans through the (531) reflection is shown in the inset of Fig. 1. Two of the individual peaks are broader and comprise two nearly overlapping reflections, and the whole sample is thus found to be made up of seven distinct crystallites that are well enough aligned to give "quasisingle" (though very broad) Bragg reflections. There are also some (lesser) misalignments about other axes that show up as extensions and splittings in the plane of the main image in Fig. 1. Despite the multicrystallite nature of the sample, it was possible to obtain accurate relative intensities by ensuring that each multireflection was integrated over a sufficient range in ω to include all seven crystallites, and using an integration "box" sufficiently wide to accommodate the extensions in the plane of the image (Fig. 1). The SMART, RLATT, GEMINI, and SAINTPLUS program suites [12] were used for indexing, integration, and data reduction. The large integration volume, and relatively low signal-to-noise and signal-to-background all tended to make the data quality poorer than for Cs-III. Nevertheless, the internal agreement factor, R_{int}, between symmetry equivalent reflections was still acceptably good at 12.9%, compared to 9.0% for the Cs-III data [9].

After removing reflections affected by Bragg reflections from the diamond anvils, and by powder lines from the tungsten gasket and beryllium backing disks of the DAC, reliable intensities were obtained for 871 reflections to a resolution of 0.9 Å. These were averaged to give 510 unique reflections, of which 470 had $F > 4\sigma(F)$. The SIR-92 [15] and SIR-97 [16] direct methods packages were both used for *ab initio* structure solution and gave the same solution. The final fit to the structure, which included anisotropic atomic displacement (thermal motion) parameters, gave an R factor ($R1$) of 19.7% for the 470 unique data with $F > 4\sigma(F)$ and a goodness of fit χ^2 of 2.50. Structure refinement was performed using SHELXL-97 [17]. The largest residual density in the Fourier difference map was $4.50e^-/\text{Å}^3$, whereas deletion of one of the Rb atoms in the refinement resulted in a difference peak of $\sim 25e^-/\text{Å}^3$. This confirms that no atoms have been omitted from the solution. All structure solving and refinement was performed via the WinGX interface [18].

The refined lattice parameters and atomic coordinates of Rb-III obtained from the single crystal at 14.3 GPa [13] are given in Table I. From the lattice parameters, we were able to index the powder-diffraction profiles and thus obtain V/V_0 as a function of pressure as shown in Fig. 2 ($V_0 = 92.74$ Å^3/atom). The volume changes at the Rb-II $\rightarrow$ Rb-III and Rb-III $\rightarrow$ Rb-IV transitions are 2.5(2)% and 0.9(1)%, respectively. The nearest-neighbor distances in Rb-IV and Rb-II extrapolated to 14.3 GPa are 3.2 [19] and 3.6 Å, respectively, and Table I gives the number of interatomic distances for each atom in the ranges <3.2 Å, 3.2–3.6 Å, and 3.6–4.1 Å. The upper bound of 4.1 Å is somewhat arbitrary but has been set, as for Cs-III [9], at the first minimum in the distribution of contact distances. Each atom is then surrounded by 8–11 others between 3.1 and 4.0 Å, giving an average coordination close to 10 as in Cs-III. The shortest Rb-Rb distance of 3.17 Å is ~ 0.1 Å longer than the shortest distance in Rb-IV extrapolated to this pressure [19], but the complex

TABLE I. Refined atomic coordinates of Rb-III at 14.3 GPa in space group $C222_1$. Rb1 occupies a fourfold 4b site, and Rb2-Rb7 occupy eightfold 8c sites. (The coordinates are referred to the standard space group origin and differ by $\frac{1}{4}$ in y from those used in Figs. 2, 3, and 4.) The refined lattice parameters are $a = 7.886(2)$ Å, $b = 11.240(2)$ Å, and $c = 18.431(2)$ Å. The number of nearest-neighbor (n-n) interatomic distances in the ranges (i) <3.2 Å, (ii) 3.2–3.6 Å, and (iii) 3.6–4.1 Å are given for each atom.

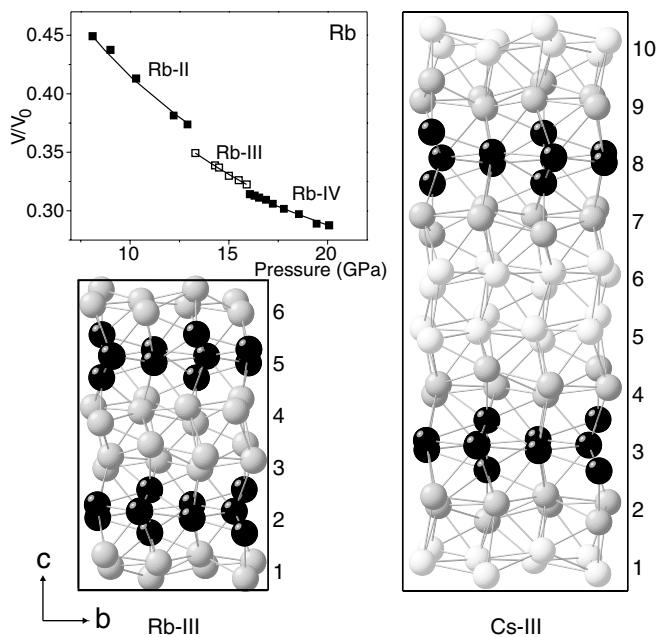| | Atomic coordinates ($\times 10^4$) | | | No. of n-n contacts | | |
	x	y	z	(i)	(ii)	(iii)
Rb1	0	745(15)	2500	0	8	2
Rb2	1955(30)	3517(19)	2699(6)	1	7	2
Rb3	1219(31)	6273(17)	3186(7)	1	7	0
Rb4	9873(19)	4196(10)	4287(6)	1	7	3
Rb5	5805(23)	3931(12)	3871(6)	0	7	4
Rb6	3602(21)	6308(9)	4639(8)	0	8	2
Rb7	7442(34)	6753(23)	4139(8)	0	7	4

FIG. 2.   Crystal structures of Rb-III and Cs-III, on the same scale, viewed along the a axis of the $C222_1$ unit cell. Rb-III is drawn with a nonstandard origin on a 2_1 screw axis along a to facilitate comparison with Cs-III which is drawn with the standard origin on a twofold axis (see text and note [20]). The 8- and 10-atom a-b layers in the two structures are numbered. Nonequivalent 8-atom layers in Cs-III are in two different shades of grey. Contact distances of up to 4.1 Å for Rb-III and 4.7 Å for Cs-III are shown as solid lines. Inset: equation of state of Rb-II, III, and IV. The lines are guides to the eye.

incommensurate nature of the Rb-IV structure obscures the meaning of this comparison.

The structure of Rb-III is shown in projection down the a axis in Fig. 2. It bears a striking resemblance to the Cs-III structure, also shown, despite the very different relative c-axis lattice parameters. Both structures can be understood in terms of similar 8- and 10-atom a-b layers stacked along c. Cs-III has ten layers: two symmetry-related 10-atom layers (shown in black), and two different sets of four symmetry-related 8-atom layers (identified using different shades of grey). Rb-III has two 10-atom layers but only one set of four 8-atom layers. It is apparent that the arrangement of atoms in layers 1, 2, 3, and 4 of Rb-III is closely similar to that in layers 2, 3, 4, and 5 of Cs-III. However, Rb-III cannot be understood as simply Cs-III with half the 8-atom layers removed—for example, it can be seen that layer 5 of Rb-III is *not* arranged exactly like layer 8 of Cs-III [20]. In fact, Rb-III is obtained from Cs-III by removing the light-grey 8-atom layers and shifting each alternate remaining 8-/10-/8-atom block $\frac{1}{2}$ in y. Hence, the coordinates in Table I are close to those of Cs1 to Cs7 in Ref. [9] except that the y coordinates differ by about $\frac{1}{4}$—and thus the origin difference adopted in Fig. 2.

The remarkable similarity between the a-b layers of the two structures is apparent in Fig. 3. As seen in projection, the 8-atom layers all have chains of slightly distorted squares inclined at about $+35°$ or $-35°$ to the b axis.
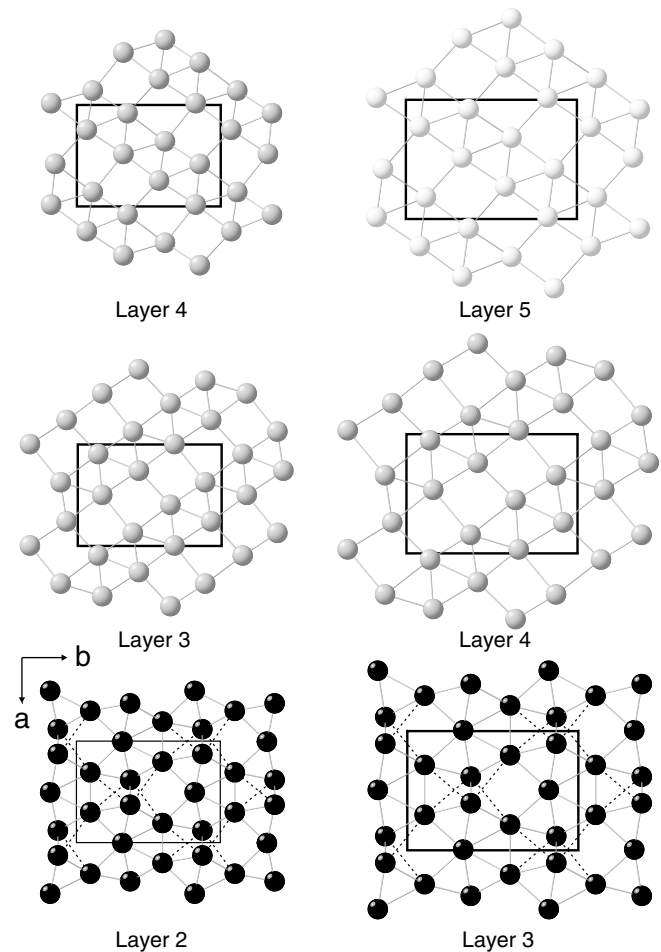
FIG. 3.   The a-b layers 2, 3, and 4 of Rb-III (left) and 3, 4, and 5 of Cs-III (right) shown on the same scale and viewed down the c axis. The unit cells are marked. The origins used and contact distances marked by solid lines are as in Fig. 2. Dotted lines in the 10-atom layers show next-nearest-neighbor contact distances in the range 4.1–4.4 Å (Rb-III) and 4.7–5.0 Å (Cs-III).

The squares are all capped at each end with triangles in a 3^34^2 arrangement in the Pearson notation [21]. We have found no other structure with this particular extended form of 3^34^2 arrangement, but similar motifs of squares and "nose-to-tail" triangles are seen in binary systems such as UAl_4, As_2Te_3, and Ni_4B_3 [21].

The 10-atom layers in the two structures are also very similar but more complex. No simple net is apparent when considering contacts up to 4.1 Å. But if the shortest next-nearest neighbor contacts are also considered (dashed lines in Fig. 3), chains of squares and triangles similar to, but considerably more distorted than, those in the 8-atom layers can be discerned, inclined at about $+35°$ *and* $-35°$ to the b axis in the same layer. These (far from planar) layers might thus be understood as an amalgam of the structural motifs of the two adjacent 8-atom layers.

Figure 4 shows one of the a-c sheets of the Rb-III structure. (These are viewed edge on, along the a axis, in Fig. 2.) The particular one drawn has a 2-atom group of the 10-atom a-b layer—the black atoms—at $z = \frac{1}{4}$ and
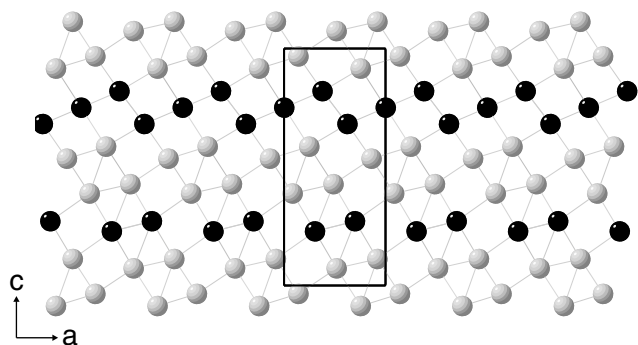
FIG. 4.   The *a-c* sheet of the Rb-III structure at $y \sim 0.35$ in Figs. 2 and 3. The unit cell is shown. Contact distances marked by solid lines are as in Fig. 2.

a 3-atom group from that layer at $z = \frac{3}{4}$ (compare Fig. 3). Around $z = \frac{3}{4}$ the atoms in this *a-c* sheet can be seen to form an almost regular square array, while around $z = \frac{1}{4}$ there is an arrangement similar to the motif of squares and "nose-to-tail" triangles in the 8-atom *a-b* layers in Fig. 3. The *a-c* sheets of Cs-III show the same features. Thus the spatial arrangement of atoms in these structures is a mixture of approximately simple square and 2-*d* close-packed in both the *a-b* and *a-c* planes.

The structures of Rb-III and Cs-III represent a remarkable new elemental structure type. All the other known structures in the alkali metals are relatively simple [1,5,22], or can be understood as distortions or superstructures of simple bcc or fcc [6,23,24]. Even the complex incommensurate Rb-IV structure is composed of quite simple "host" and "guest" components [4]. Rb-III and Cs-III open up an altogether higher level of structural complexity in alkali metals that needs to be understood. The very narrow range of stability for Cs-III of only 0.05 GPa might have made this structure seem a rare oddity. But the substantial range of 3 GPa (and ~9% variation in density; see Fig. 2) in Rb-III establishes the structural significance of this complex arrangement. Rb-III is the simplest structure with both types of layer. It is conceivable that there could be a structure like Rb-III but with a second 10-atom layer between neighboring 8-atom layers; this would give 72 atoms in the unit cell. Cs-III is the next possibility, and there may be even more complex stackings possible beyond that.

One of the more surprising discoveries in metals recently has been the modulated self-incommensurate structures in Ba, Rb, and several other elements, comprising interpenetrating host and guest components [4,25–27]. The stacking of different proportions of layers of different thickness in Rb-III and Cs-III can be considered as another form of modulation, and it would be of great interest to carry out calculations of possible stacking sequences to explore further this intriguing aspect of these new structures.

[1] D. A. Young, *Phase Diagrams of the Elements* (University of California Press, Berkeley, CA, 1991), and references therein.

[2] H. T. Hall, L. Merrill, and J. D. Barnett, Science **146**, 1297 (1964).

[3] See Ref. [9] and references therein.

[4] M. I. McMahon, S. Rekhi, and R. J. Nelmes, Phys. Rev. Lett. **87**, 055501 (2001).

[5] H. Olijnyk and W. B. Holzapfel, Phys. Lett. **99A**, 381 (1983).

[6] U. Schwarz *et al.,* Solid State Commun. **112**, 319 (1999).

[7] M. Winzenick, V. Vijayakumar, and W. B. Holzapfel, Phys. Rev. B **50**, 12 381 (1994).

[8] U. Schwarz *et al.,* Phys. Rev. Lett. **83**, 4085 (1999).

[9] M. I. McMahon, R. J. Nelmes, and S. Rekhi, Phys. Rev. Lett. **87**, 255502 (2001).

[10] H. K. Mao, J. Xu, and P. M. Bell, J. Geophys. Res. **91**, 4673 (1986).

[11] R. J. Nelmes and M. I. McMahon, J. Synchrotron Radiat. **1**, 69 (1994).

[12] Brucker AXS Inc., Madison, WI.

[13] No ruby signal was observable from this sample. The pressure was subsequently determined to be 14.3 GPa using the equation of state of Rb-III obtained from the powder data.

[14] R. J. Cernik *et al.,* J. Synchrotron Radiat. **4**, 279 (1997).

[15] A. Altomare *et al.,* J. Appl. Crystallogr. **26**, 343 (1993).

[16] A. Altomare *et al.,* J. Appl. Crystallogr. **32**, 115 (1999).

[17] SHELXL-97 — A program for single crystal structure refinement. G. M. Sheldrick, University of Goettingen, 1997.

[18] L. G. Farrugia, J. Appl. Crystallogr. **32**, 837 (1999).

[19] This value of 3.2 Å is the average of the shortest nearest-neighbor distances in the host and guest components of the incommensurate Rb-IV structure; see Ref. [4].

[20] Figure 3 reveals that although layers 4 and 5 of Cs-III are not symmetry related, they are only slightly distorted from being related by the same operators as between layers 5 and 6 *but displaced $\frac{1}{4}$ in y*. The same pseudosymmetry relates layers 1 and 2. These pseudosymmetry operators become the true symmetry between layers 3 and 4 (and between layer 1 and layer 6 of the adjacent unit cell) in Rb-III. The difference between layer 5 of Rb-III and layer 8 of Cs-III thus arises because, whereas (for example) the group of three atoms at $y \sim 0.35$ in Rb-III layer 2 is related to the corresponding group at $y \sim 0.65$ in layer 5 by a 2_1 screw axis along x at $y = \frac{1}{2}$ and $z = \frac{1}{2}$, the equivalent two groups in Cs-III are related by a twofold axis.

[21] W. B. Pearson, *The Crystal Chemistry and Physics of Metals and Alloys* (Wiley-Interscience, New York, 1972).

[22] K. Takemura, S. Minomura, and O. Shimomura, Phys. Rev. Lett. **49**, 1772 (1982).

[23] U. Schwarz *et al.,* Phys. Rev. Lett. **81**, 2711 (1998).

[24] M. Hanfland *et al.,* Nature (London) **408**, 174 (2000).

[25] R. J. Nelmes *et al.,* Phys. Rev. Lett. **83**, 4081 (1999).

[26] M. I. McMahon *et al.,* Phys. Rev. B **61**, 3135 (2000).

[27] M. I. McMahon, O. Degtyareva, and R. J. Nelmes, Phys. Rev. Lett. **85**, 4896 (2000).